DALTON
FULL PAPER

Vibrational modes and structure of liquid and gaseous zirconium tetrachloride and of molten $ZrCl_4$–CsCl mixtures ‡

G. M. Photiadis and G. N. Papatheodorou *,†

Institute of Chemical Engineering and High Temperature Chemical Processes—FORTH, and Department of Chemical Engineering, University of Patras, PO Box 1414, GR-26500, Patras, Greece

Raman spectra of liquid and gaseous zirconium tetrachloride and of molten $ZrCl_4$–CsCl mixtures have been measured. Changes of the relative Raman intensities in the vapor phase, near and above the critical point, have established the dimerization reaction $2ZrCl_4(g) \rightleftharpoons Zr_2Cl_8(g)$, $\Delta H_R = -56.6 \pm 1.1$ kJ mol^{-1}. Spectra of solid and molten zirconium chloride show that in the liquid phase $ZrCl_4$ monomers are present in equilibrium with polymer-like $(ZrCl_4)_n$ species. A systematic investigation of the Raman spectra of the solid mixtures formed upon cooling the $ZrCl_4$–CsCl melts at different compositions has shown that apart from the known Cs_2ZrCl_6 a new compound with stoichiometry $CsZr_2Cl_9$ is also formed. The spectra of solid and molten Cs_2ZrCl_6 and $CsZr_2Cl_9$ show that $ZrCl_6^{2-}$ and the $Zr_2Cl_9^-$ are present in both phases. In molten $ZrCl_4$–CsCl mixtures and at compositions $x_{ZrCl_4} < 0.33$ the $ZrCl_6^{2-}$ octahedra are predominant. In the range $0.33 < x_{ZrCl_4} < 0.66$ the spectral changes with temperature and composition reflect an equilibrium involving three ionic species: $ZrCl_6^{2-}$, $Zr_2Cl_9^-$ and $Zr_2Cl_{10}^{2-}$ (or $ZrCl_5^-$). At mole fractions rich in $ZrCl_4$ ($x_{ZrCl_4} > 0.66$) the spectra indicate an equilibrium between the ionic $Zr_2Cl_9^-$, the $ZrCl_4$ monomer and the $(ZrCl_4)_n$ polymer-like species. All data suggest that the value of n is small and most probably hexamers and/or dimers are the predominant 'polymer' species in these melts.

The examination of the vibrational Raman spectra of mixtures of metal halides MX_n ($n = 2, 3, \ldots$) with alkali-metal halides in the molten state has provided a means of identifying the species that may exist in the melt and indirectly has given information regarding the liquid structure of the MX_n pure component.[1] Extensive studies have been reported for systems involving divalent (*e.g.* MgX_2,[1] ZnX_2,[2] $HgCl_2$,[3] $CdCl_2$,[1] $MnCl_2$,[1] *etc.*) and trivalent (*e.g.* AlF_3,[1] $AlCl_3$,[1] BF_3,[1] YCl_3,[4] $NdCl_3$,[5] *etc.*) metal halides, whilst studies involving tetra- or penta-valent halides are very limited.[1] Exceptions are the mixtures involving zirconium tetrahalides which have been investigated by different groups of researchers over the past twenty-five years. The early Raman work of Toth *et al.*[6] has established the presence of 'octahedral' ZrF_6^{2-} species in molten mixtures rich in LiF–KF; similarly $ZrCl_6^{2-}$ species were inferred in melts with composition A_2ZrCl_6 (A = Na, K or Cs).[7] A comparison of the solid- and liquid-state spectra of pure $ZrCl_4$ indicates that the 'polymeric' like chains present in the solid[8] are also preserved in the melt.[9–11]

The purpose of the present work is to investigate the structural properties of molten $ZrCl_4$ and its mixtures with CsCl. Careful measurements of the temperature and composition effects on the Raman spectra of these melts as well as spectral changes occurring upon melting the crystalline binary compounds formed in the $ZrCl_4$–CsCl binary are used to identify the different species present. Caesium chloride was chosen as the solvent melt due to the increased stability, relative to the lighter alkali-metal chlorides, that the Cs^+ cation offers to the different species formed in melt mixtures.[1] Furthermore, quantitative Raman spectroscopic measurements on pure $ZnCl_4$ near and above the critical point ($t_c = 503.5$ °C, $P_c = 57.4$ atm) are used to establish the structure and the degree of 'polymerization' in the vapor and liquid phases.

From an applied viewpoint, dilute solutions of $ZrCl_4$ in alkali-metal halide solvents have been considered for the electrorefining of Zr metal.[12,13] Molten-salt electrolysis for the production of Zr metal appears to be an alternative to the expensive, batch-type metallothermic Kroll[14] process.

Experimental

Zirconium tetrachloride of practical grade (Fluka; >98% in Cl, >95% in Zr) was initially dried under high vacuum (≈10^{-6} Torr) by gradually raising the temperature to ≈150 °C for 1 d. This step was followed by slow triple sublimation at ≈230 °C under static vacuum (≈0.05 Torr) in sealed Pyrex tubes. Caesium chloride (Cerac, 99.9%) was distilled under high dynamic vacuum (≈10^{-6} Torr) at 700 °C.

The chemicals were very sensitive to moisture and were handled in a controlled nitrogen atmosphere dry-box (water content <1 ppm) or in sealed glass tubes. Thick walled fused-silica tubing (inside diameter 2 mm, outside diameter 4 mm) was used for making the Raman cells for the $ZrCl_4$–CsCl mixtures, the $ZrCl_4$ liquid and the supercritical fluid. These cells could withstand pressures even above 200 atm. A total amount of ≈200 mg was added to the cells and the mixing of the salts was achieved in the sealed cells by carefully raising the temperature and melting the salts. The cells were sealed in such a way that after melting the liquid mixtures occupied most of the cell volume. This procedure minimizes the volume over the melt and ensures no changes in the melt composition due to vaporization of $ZrCl_4$. For measuring the gas-phase spectra at pressures less than 200 atm fused-silica cells (inside diameter 9 mm, outside diameter 12 mm) were used. For the determination of the extent and enthalpy of association of gaseous $ZrCl_4$ the appropriate amounts of chemicals were loaded into known volume Raman cells for quantitative measurements as previously reported.[15]

The Raman equipment and furnace were as previously described.[15] Raman spectra were obtained from samples using the 488 nm line of an Ar^+ laser. Melts and gases were studied using two polarizations of the incident-scattered light, the horizontal–vertical (HV) and the vertical–vertical (VV). Polycrystalline solids were measured with the 'unpolarized'-vertical (UV) configuration. No impurity fluorescence bands and fluorescence background were found in the spectra.

† E-Mail: gpap@iceht.forth.gr

‡ *Non-SI units employed*: atm = 101 325 Pa, Torr ≈ 133 Pa; P = 10^{-1} Pa s.

Table 1 Observed Raman bands (in cm^{-1}) and assignments for the three phases of $ZrCl_4$

Solid			Liquid		Gas	
25 °C	430 °C	Assignment [a]	450–490 °C	Assignment [b]	420–600 °C	Assignment [c]
					418dp	M, ν_3
411	405	A_g, ν_t	404p	P_L, ν_{t_1}	404p	D, ν_t
393	385	B_g	398dp	P_L		
			375p	M, ν_1	375p	M, ν_1
308	302	B_g	(340p) [d]	P_L	310p	D, ν_b
283	277	A_g, ν_{b_1}	295p	P_L, ν_b		
220		A_g, B_g, ν_{b_2}				
142	140	A_g	(120dp)	P_L		
			107dp	M, ν_2, ν_4	≈100dp	M, ν_2, ν_4
132	127	B_g				
102		B_g				
94	89	A_g	80dp	P_L		
82		B_g				
77	71	A_g	(71dp)	P_L		

[a] Ref. 17. [b] P_L = 'Polymer', $(ZrCl_4)_n$; M = monomer, $ZrCl_4$. [c] D = Dimer, Zr_2Cl_8; D_{2h} symmetry. [d] Parentheses indicate weak shoulder bands.

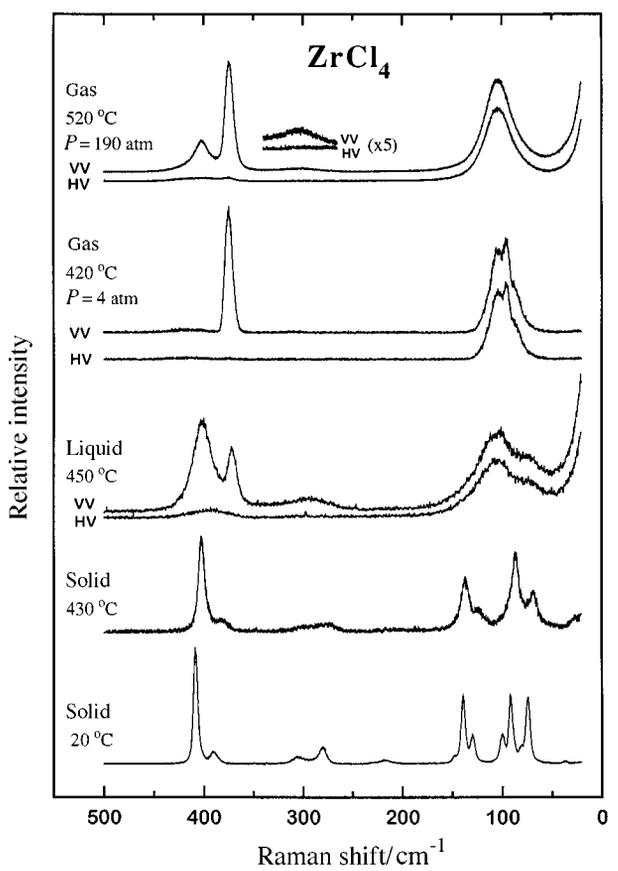

Fig. 1 Raman spectra of solid, liquid and gaseous $ZrCl_4$. Conditions: λ_0 = 488 nm, power = 100 mW, slits 3 cm^{-1}, time constant 0.1 s, scan rate 1 cm^{-1} s^{-1}. For the gas-phase spectra: power = 300 mW, slits 5 cm^{-1} s^{-1}

Results and Discussion

Vibrational modes and phase transitions of pure $ZrCl_4$

The vapor pressure of solid $ZrCl_4$ near its melting point at 437 °C is about 19 atm.[16] The pressure over the liquid increases rather rapidly reaching ≈57 atm at the critical temperature (t_c = 503 °C). Raman spectra were measured for the three phases at different temperatures and pressures and typical results are shown in Fig. 1. The frequencies and polarization characteristics of the observed bands are listed in Table 1. It was further observed that at elevated pressures the relative intensities of the Raman bands in the liquid and gaseous phases changed reversibly with temperature and/or pressure. This behavior indicated that different species in equilibrium may exist in the two phases and thus, quantitative Raman spectral measurements[15] were necessary in order to identify and characterize these species.

Dimerization in the gas phase above and below the critical point. Mass spectrometric[16] and Raman spectroscopic[18] measurements have established that monomeric tetrahedra are the main species in the $ZrCl_4$ vapors. However, the existence of low partial pressure dimers has been argued from the mass spectrometric measurements. The vapor Raman spectrum (Fig. 1) obtained at ≈4 atm pressure shows only the expected $ZrCl_4$ tetrahedron vibrational frequencies ν_1 at 377 cm^{-1} and ν_3 at 418 cm^{-1} as well as the vibrational rotational contours[18] for the $\nu_2(E)$ and $\nu_4(F_2)$ modes around 100 cm^{-1}. At this pressure no Raman band due to other species could be observed. However, the spectra of the saturated vapor over the liquid at temperatures above 450 °C showed an additional band ν_1* at ≈404 cm^{-1}. With the liquid always present, the intensity of the ν_1* band of the saturated vapor increased with increasing temperature relative to the ν_1 band of the $ZrCl_4$(g). Measurements of the vapors over the liquid at 450, 470 and 490 °C, where the vapor pressures were approximately 25, 35 and 47 atm respectively, almost doubled the intensity of the ν_1* band. This behavior suggests association in the gas phase according to reaction (1).

$$n\mathrm{ZrCl_4(g)} \rightleftharpoons \mathrm{Zr}_n\mathrm{Cl}_{4n}\mathrm{(g)} \quad (1)$$

Presumably increasing pressure favors the association and thus the new ν_1* band is assigned to the Zr_nCl_{4n}(g) species. The stoichiometry and thermodynamics of the gas-phase reaction can be determined by quantitative Raman intensity measurements as described in detail in ref. 15. The integrated Raman band intensities I_M and I_D of the monomer and associated species respectively are related to the concentrations c_M and c_D of the species present and the concentration equilibrium constant K_c; equations (2a) and (2b). The stoichiometry coefficient n can be

$$I_i(\nu) = F(\nu, T)C_i \quad (i = \mathrm{M\ or\ D}) \quad (2a)$$

$$K_c = \frac{C_D}{C_M{}^n} \propto K_I = \frac{I_D}{I_M{}^n} \quad (2b)$$

determined by measuring K_I at two different total pressures P and P' at the same temperature under the assumption that K_I and K_c are pressure independent, equation (3), where I_M, I_D and

$$n = \frac{\ln(I_D/I'_D)}{\ln(I_M/I'_M)} \quad (3)$$

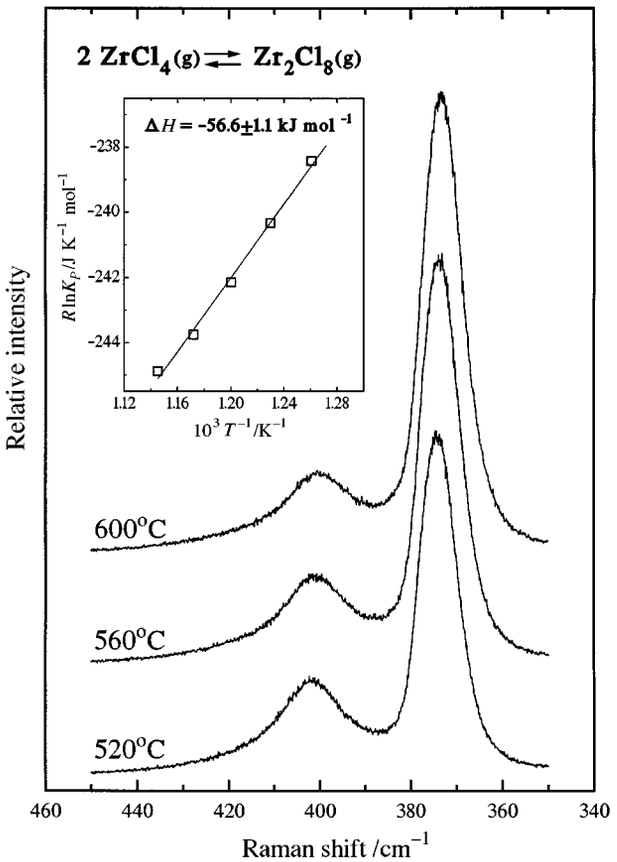

Fig. 2 Raman spectra (polarized VV) of supercritical $ZrCl_4$ fluid in the region of ν_1 and ν_t. Conditions as in Fig. 1. Insert: plot of $R \ln K_P$ *vs.* $1/T$ for the dimerization reaction

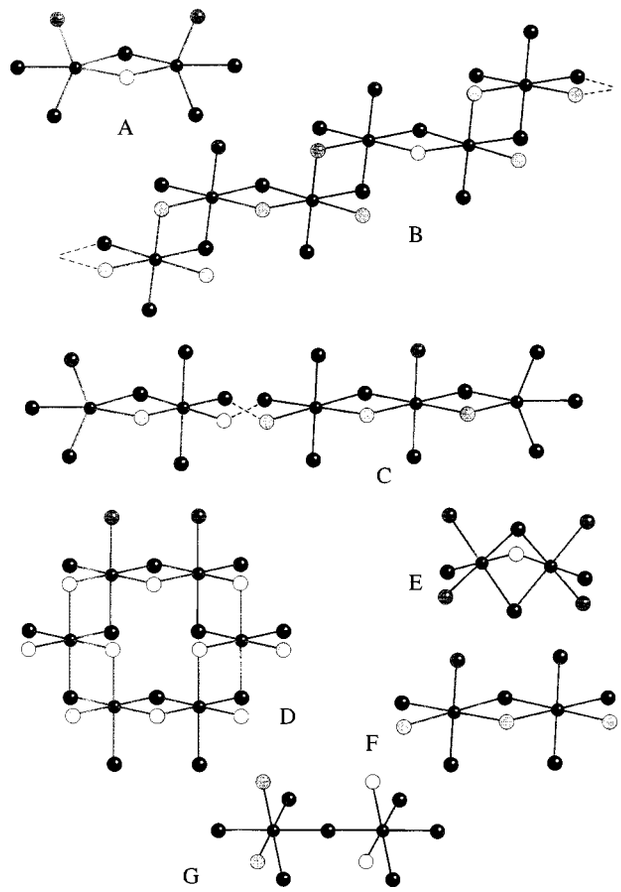

Fig. 3 Models for zirconium(IV) chloride structures. **A**, dimer Zr_2Cl_8; **B**, zigzag chains in solid $[(ZrCl_{4/2})Cl_2]_n$; **C**, chain molecule with octahedra bridged by equatorial chlorines $[(ZrCl_{4/2})Cl_2]_n(ZrCl_3)_2$; **D**, zigzag octahedra in the hexamer Zr_6Cl_{24}; **E**, face-sharing bioctahedral ion $Zr_2Cl_9^-$; **F**, edge-sharing bioctahedral ion $Zr_2Cl_{10}^{2-}$; **G**, apex-sharing bioctahedral ion $Zr_2Cl_{11}^{3-}$

I'_M, I'_D are the Raman intensities measured from cells with total pressures P and P' respectively. Assuming 'ideal gas' behavior, the equilibrium constant $K_P = (RT)^{(1-n)}K_c$ and the enthalpy of reaction (1) can be determined from a Van't Hoff-like plot, equation (4).

$$R \ln K_P = -(\Delta H°/T) + \text{constant} \qquad (4)$$

Vapor density measurements have shown that $ZrCl_4$(g) deviates from ideal gas behavior, having a compressibility factor ($Z = PV/RT$) less than one at temperatures above 380 °C.[19–21] Thus, the use and application of equations (3) and (4) for the present system is questionable. The deviation however of equation (3) assumes a pressure-independent K_c (or K_I) and does not imply ideal gas behavior. The use of equation (3) for the experimental determination of n requires that no condensed phase (liquid) $ZnCl_4$ is present in the cell. In addition, in order to have meaningful quantitative measurements, the intensities I_M and I_D should be easily measurable and comparable. This was achieved by making measurements at temperatures above the critical point of $ZrCl_4$. Thick walled fused-silica cells of known volume were loaded with $ZrCl_4$ having at 550 °C a calculated (as monomer) 'ideal gas' pressure of ≈90 to 190 atm and thus the relative Raman intensities were measured in the supercritical fluid. Fig. 2 shows the temperature effect on ν_1 and ν_1*. The values of n calculated from equation (3) by combining the three experiments were 1.93, 2.09 and 1.99 giving an average of $n = 2.0 \pm 0.1$ for $T \approx 550$ °C which implies that the new gaseous species is the Zr_2Cl_8 dimer. Presumably the structure of the dimer is as shown in **A** in Fig. 3 having its strong polarized vibrational mode ν_1* at ≈404 cm^{-1} close to the terminal Zr–Cl_t frequency ν_1 at 401 cm^{-1} measured for the $ZrAlCl_7$ vapor complex.[15] In both molecules the Zr is five-co-ordinate having three terminal and two bridging bonds. A tentative assignment of the Raman bands observed in the 'gaseous' dimer–monomer spectra is given in Table 1.

The approximate determination of the enthalpy of reaction (1) according to equation (4) and to the Van't Hoff plot (insert, Fig. 2) gives $\Delta H_D = -56.6 \pm 1.1$ kJ mol^{-1}, close to that found[16] by mass spectrometric studies ($\Delta H = -55$ kJ mol^{-1}).

The melting of the solid and the liquid structure. Crystalline zirconium tetrachloride is monoclinic with a $P2/c$ (C_{2h}^4) space group having two molecules per unit cell.[8] The zirconium atom has a C_2 site symmetry in a structure characterized by zigzag polymer chains $[(ZrCl_{4/2})Cl_2]_n$ of bridged octahedra. The edge-sharing octahedra are very distorted leading to three pairs of distinct Zr–Cl bonds; two types of bridging and one terminal bond have Zr–Cl distances of 2.655, 2.498 and 2.307 Å respectively. This chain polymer-like structure (Fig. 3, **B**) has been considered to represent a transition from the mainly molecular $TiCl_4$ to the more ionic MCl_3 (M = rare-earth metal).[8]

The room-temperature Raman spectra of crystalline $ZrCl_4$ (Fig. 1 and Table 1) are in agreement with the spectra reported and analyzed by Taylor *et al.*[17] Twelve Raman-active internal modes are expected for the solid, $\Gamma_{int} = 6A_g + 6B_g$, and their assignment based on normal coordinate analysis[17] is given in Table 1. The terminal Zr–Cl_t frequency at ≈411 cm^{-1} is close to the analogous terminal frequency (≈412 cm^{-1}) of the vapor complex $ZrAl_2Cl_8$ in which Zr has a six-fold co-ordination.[15] The bands at 283 and 220 cm^{-1} have been assigned[17] to the two different types of bridging Zr–Cl_b bonds. The main spectral characteristics of solid $ZrCl_4$ do not change with increasing temperature: all bands became broader and shift to lower energies (Fig. 1 and Table 1). At 430 °C, just below melting,

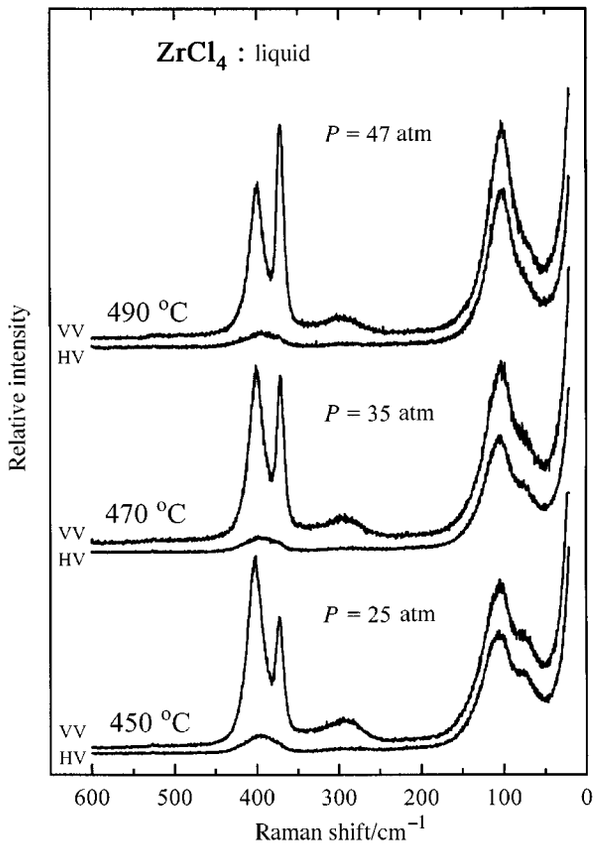

Fig. 4 Temperature dependence of the Raman spectra of molten $ZrCl_4$. Conditions as in Fig. 1; P is the vapor pressure above the liquid

seven bands are clearly seen. Upon melting, most of these modes appear to be transferred into the liquid. The deformation modes of the solid occurring in the 50–150 cm^{-1} region follow the 'red shift' trends of the solid and appear in the liquid as broad and depolarized bands. The behavior of the terminal high-frequency polarized band ν_t at 410 cm^{-1} is similar. In contrast the ν_{b_1} band at ≈277 cm^{-1} upon melting shifts to higher energies giving a polarized band at ≈295 cm^{-1}. Finally a new high-intensity polarized band appears in the spectra the frequency of which at 375 cm^{-1} is presumably that of the ν_1^M band of the $ZrCl_4$ tetrahedra, indicating that monomers are also present in the liquid.

A comparison of the solid and liquid spectra with the high-density (supercritical) vapor spectra (Fig. 2) suggests that at least two different types of species are predominant in the liquid phase. Monomeric $ZrCl_4$ with a main polarized band at 375 cm^{-1} and 'polymeric like' species with a main polarized band at 404 cm^{-1}. The proximity of the frequency of the latter band to the terminal frequency ν_t of both the Zr_2Cl_8 gaseous dimer and of the $[(ZrCl_{4/2})Cl_2]_n$ chain in the solid cannot be used to characterize the size and the structure of the 'polymeric' species. Measurement of the liquid-phase spectra at different temperatures (Fig. 4) confirms the presence of the monomers and suggest that an equilibrium of the type (5) may exist in the melt.

$$(ZrCl_4)_n(l) \rightleftharpoons nZrCl_4(l) \qquad (5)$$

The structure of the polymeric species may be analogous to the zigzag octahedral chains existing in the solid (Fig. 3, **B**) but having also two end zirconium atoms in a five-fold co-ordination as in the dimer, *e.g.* $[(ZrCl_{4/2})Cl_2]_n(ZrCl_3)_2$. A similar chain may be formed with the octahedra bridged by the equatorial chlorines as shown in **C**. Ring structures are also possible but these would have a tendency to distort the octahedral angles unless n is very large. An exception is the symmetrical ring structure Zr_6Cl_{24} (Fig. 3, **D**) having the zirconium atoms in the middle of six connected edges of a cube and thus forming a closed zigzag structure of octahedra with bridging chlorides both at six apexes and at the center of six faces of the cube.

Table 2 Properties of solid and liquid $ZrCl_4$

	Density ($g\ cm^{-3}$)	Molar volume ($cm^3\ mol^{-1}$)	Viscosity (cP)	Ref.
Solid (25 °C)	2.8	83		8
Liquid (440 °C)	1.61	145	0.38	20, 21
(490 °C)	1.22	191	0.14	20, 21

The chemical equilibrium methods used in deriving equation (3) in order to calculate the value of n in the vapor phase are not applicable for the liquid and the extent of polymerization cannot be calculated. It is evident however from the properties of the solid and the liquid listed in Table 2 that the melt is rather molecular. Upon melting a large volume expansion (≈77%) occurs and a high-fluidity non-conducting liquid is formed. With increasing temperature the liquid continues to expand drastically and its fluidity increases (Table 2). All these observations are consistent with the above equilibrium and furthermore indicate that the polymerization (value of n) in the melt is rather small and more likely the molecular liquid is composed of either Zr_2Cl_8 dimers, as in the vapor phase, or Zr_6Cl_{24} hexamers in equilibrium with monomers.

The assignments of all the bands observed in the liquid spectra are given in Table 1. The 'polymer' species and the high-temperature solid have bands with similar frequencies and relative intensities. A comparison of the temperature dependence of the spectra in Figs. 2 and 4 indicates that small variations of temperature increase more rapidly the monomer intensity, relative to that of the 'polymer' or dimer, in the liquid (Fig. 4) than in the vapor (Fig. 2). This would imply that n is higher in the liquid than in the vapor (where $n = 2$) and further supports the presence of the hexamer molecules in the melt.

Finally, for the assignments in Table 1 it should be pointed out that: (a) the two types of bridging frequencies in the solid[17] at 283 and 220 cm^{-1} become equivalent in the liquid giving rise to the 295 cm^{-1} polarized band; (b) independent of the ring (*e.g.* Fig. 3, **D**) or the chain (*e.g.* Fig. 3, **C**) structure that the $(ZrCl_4)_n$ may have, there will always be octahedral terminal bonds $Zr–Cl_t$ (two per Zr atom) and bridging bond $Zr–Cl_b$ (four per Zr atom). Furthermore, if the structure is open then there will be two additional types of $Zr–Cl_t$ terminal bonds at the end of the chain where the Zr is five-co-ordinated. As in the dimer, two terminal bonds are equivalent lying on a plane perpendicular to the $Zr(\mu\text{-}Cl)_2Zr$ plane while the third $Zr–Cl_t$ bond lies on the latter plane.

Changes of vibrational modes upon melting Cs_2ZrCl_6 and $CsZr_2Cl_9$

The phase diagram of the $ZrCl_4$–CsCl system[22,23] shows the formation of only one binary compound with stoichiometry Cs_2ZrCl_6 which melts congruently at ≈805 °C. Two eutectic mixtures are formed at mole fraction x_{ZrCl_4} ≈0.15 and 0.67 with melting temperatures 588[23] and 286 °C[22] respectively. The systematics however of the $ZrCl_4$–ACl (A = Na, K or Cs) binaries[24] indicate that other incongruently melting compounds like $AZrCl_5$ and AZr_2Cl_9 might also be present. We have examined this possibility by studying the Raman spectra of the $ZrCl_4$–CsCl solid mixtures formed by cooling a series of melt mixtures with compositions $0.05 \leqslant x_{ZrCl_4} \leqslant 1.0$.

It was observed that: (i) at $x_{ZrCl_4} \leqslant 0.33$ the solidified mixtures gave spectra due to the Cs_2ZrCl_6 ($x = 0.33$) compound as seen in Fig. 5; (ii) at $0.33 < x_{ZrCl_4} < 0.66$ the spectra of the solidified mixtures were a superposition of bands due to

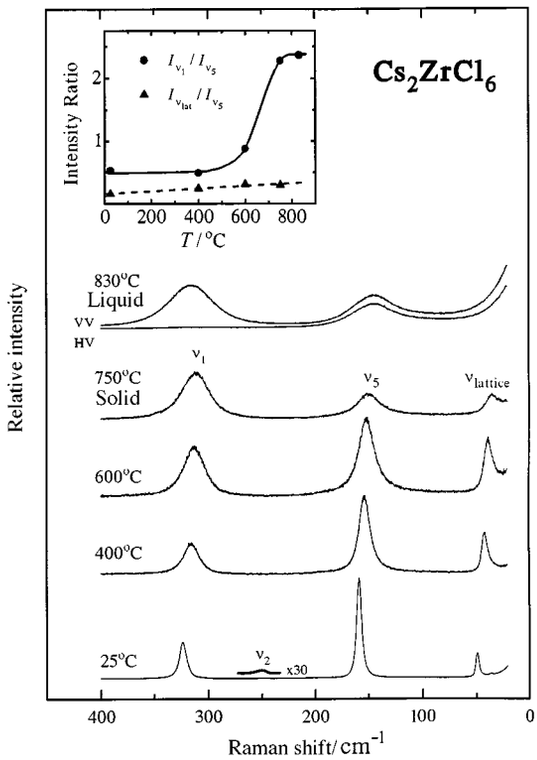

Fig. 5 Raman spectra of polycrystalline and molten Cs_2ZrCl_6. Conditions as in Fig. 1. Insert: plot of intensity ratios of the main peaks *vs.* temperature

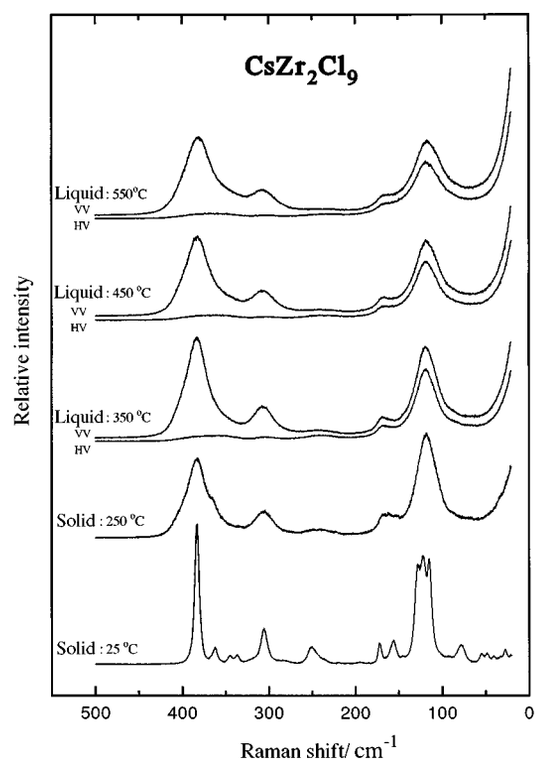

Fig. 6 Raman spectra of solid and molten $CsZr_2Cl_9$. Conditions as in Fig. 1

Cs_2ZrCl_6 plus a new solid compound. At $x = 0.66$ only bands due to the new compound were seen (Fig. 6); (iii) at $0.66 < x_{ZrCl_4} < 1.0$ the solid spectra were characterized by overlapping bands of $ZrCl_4$ (Fig. 1) and of the new compound. All these observations have shown that the $CsZr_2Cl_9$ ($x_{ZrCl_4} = 0.66$) solid compound is formed in the binary with an incongruent melting point near the eutectic temperature (≈280 °C).

Table 3 Assignments of the Raman bands (cm^{-1})[a] of solid and liquid Cs_2ZrCl_6

T/°C	$\nu_1(A_{1g})$	$I(\nu_1)$[b]	$\nu_5(F_{2g})$	$I(\nu_5)$	$\nu_L(F_{2g})$	$I(\nu_L)$
25[c]	325	100	161	200	51	30
200	322	150	158	300	48	70
400	319	200	157	430	45	100
600	315	440	155	520	42	150
750	314	500	153	240	37	70
830 (melt)	319p	700	147dp	310		

[a] The frequencies extrapolated to ≈0 K satisfy the relation:[4] $\nu_1^2 = \nu_2^2 + \frac{3}{2}\nu_5^2$. [b] $I(\nu_i)$ are the integrated relative Raman intensities. [c] $\nu_2(E_g)$ 252 cm^{-1}, $I(\nu_2)$ 5.

Cs_2ZrCl_6. The crystal structure of Cs_2ZrCl_6 has cubic $Fm3m$ (O_h^5) symmetry with the zirconium atom at an octahedral O_h site.[25] A factor-group analysis[4] for this type of compound predicts and identifies four Raman-active modes: $\Gamma_{Raman} = \Gamma_{internal} + \Gamma_{lattice}$; $\Gamma_{internal} = A_{1g} + E_g + F_{2g}$; $\Gamma_{lattice} = F_{2g}$. The internal vibrations are those of the $ZrCl_6^{2-}$ octahedra and the lattice mode is due to the translatory motion of Cs^+. The Raman spectra of Cs_2ZrCl_6 from the room-temperature polycrystalline solid to the melt at 830 °C are shown in Fig. 5. All four predicted Raman bands are present and their frequencies with assignments are given in Table 3. Our data are consistent with the previous measurement of the room-temperature solid[26] and the melt.[7] An exception is the $\nu_L(F_{2g})$ and the weak $\nu_2(E_g)$ modes of the room-temperature solid which are seen here for the first time.

The effect of temperature on the $\nu_1(A_1)$ stretching, the $\nu_5(F_{2g})$ bending and the $\nu_L(F_{2g})$ lattice modes is similar to that observed for a series of elpasolite compounds Cs_2NaMCl_6 (M = Y, La or Nd).[4,5,27] A softening of all three modes is observed with increasing temperature. For the solid at room temperatures the intensity $I(\nu_1)$ is smaller than that of $I(\nu_5)$, but at elevated temperatures an inversion of the relative intensities occurs. Upon melting the lattice mode ν_L disappears and is replaced by the depolarized liquid (Rayleigh) wing, while the ν_1 and ν_5 octahedral modes of the solid are transferred into the melt. Both bands are broader in the melt, relative to the high-temperature solid, and their energies are shifted to higher (for ν_1) and to lower (for ν_5) frequencies. The changes and frequency shifts are similar to those observed upon melting other isostructural O_h^5 solids[4,5,27] and support the view that the $ZrCl_6^{2-}$ octahedra identified in the solid are also present in the melt.

The variation of the relative intensities $I(\nu_1)/I(\nu_5)$ and $I(\nu_L)/I(\nu_5)$ of the Cs_2ZrCl_6 with temperature is shown in the insert of Fig. 5. It should be noted that the Raman intensities of a large number of MX_6 octahedral molecules and ions follow the order $I(\nu_1) > I(\nu_5)$.[28–30] The opposite order however has been found for a series of octahedra formed in the solid compounds Cs_2NaYCl_6,[4] Cs_3YCl_6,[4] K_3YCl_6,[4] Cs_2NaMCl_6 (M = Nd[5] or La[27]), Cs_2NaMBr_6 (M = Y or Gd[31,32]) and K_3YF_6.[32] Upon melting these compounds an inversion of the $I(\nu_1)/I(\nu_5)$ relative intensity ratio occurs. The Cs_2ZrCl_6 solid follows up to ≈600 °C the order $I(\nu_1) < I(\nu_5)$, as for all the above solids, but a continuous inversion occurs between 500 and 700 °C and the solid at ≈50 °C below melting shows $I(\nu_1) > I(\nu_5)$, an order that is also kept upon melting. In the same temperature range the relative intensities of the lattice to the ν_5 mode do not change. Correction of the intensities with the thermal Bose factor $[n(\omega) + 1]$[1,32] alters slightly the intensity ratios at elevated temperatures but the overall behavior is as shown for the uncorrected results in Fig. 5 (and insert). With increasing temperature a wider distribution of the stretching (ν_1) and bending (ν_5) energies of the octahedra occur and thus the bandwidth increases for both vibrational modes. There is no obvious account for the inversion of the $I(\nu_1)$, $I(\nu_5)$ intensities of the solid. It seems that between 550 and 650 °C a premelting second-order-like transi-

Table 4 Observed Raman bands (cm^{-1}) of $CsZr_2Cl_9$ and assignments

Solid (room temperature)	Solid (250 °C)	Melt (350 °C)	Assignments to $Zr_2Cl_9^{2-}$
	410 (sh)w	410w (sh)p?	
383vs	380s	381s, p	$\nu_1(A'_1)$ terminal str.
362w	365w (sh)	363w (sh)dp	$\nu_3(E')$ terminal str.
345w			
337w			
306m	310m	305m, p	$\nu_2(A'_1)$ bridging str.
285vw			
251m	250w	240vw, dp	$\nu_g(E')$
238w (sh)			
190vw			
172m	(170m)	[167m (sh)dp]	$\nu_{15}(E'')$
156m	(155m)	[155m (sh)dp]	$\nu_{11}(E')$
128s			
122s	120s	117s, dp	$\nu_{16}(E'')$, $\nu_{12}(E')$
115s			

tion occurs which retains the 'isolated' $ZrCl_6^{2-}$ octahedra and facilitates the polarizability changes induced by the ν_1 'breathing' mode. Furthermore, the constant $I(\nu_L)/I(\nu_5)$ ratio indicates that the lattice ν_L mode (*i.e.* the Cs^+ translatory mode) is more coupled to the equatorial bending mode (ν_5) than the ν_1 mode. This could suggest a premelting phase where layers are formed involving the equatorial chlorides of the octahedra and the Cs^+ ions. Within the layer the polarizability changes induced by the ν_5 mode are inhibited relative to the changes induced by the breathing vibrations of the 'axial' chlorides. The similarity of the relative intensity ratios of the melt and the high-temperature solid would thus imply that the Cs^+ ions in the melt are also influencing the equatorial mode of the $ZrCl_6^{2-}$ octahedral ions.

$CsZr_2Cl_9$. The existence of bimetal complexes of the type $M_2X_9^{n-}$ (M = Ti,[33–35] Cr,[36,37] Tl,[38] Zr,[39,40] W[41] or Sc;[42] X = Cl, Br or I; $n = 1$ or 3) is well documented. X-Ray studies of the solid compounds $Cs_3Cr_2Cl_9$,[37] $[TeBr_3][Zr_2Br_9]$[39] and $[PPh_4][Zr_2Cl_9]$[40] have established the formation of face-sharing bioctahedra having three terminal and three bridged (by a face) halides as seen in Fig. 3, **E**. Single-crystal Raman spectra of $A_3Cr_2Cl_9$ (A = K, Rb or Cs)[36] and $Cs_3Tl_2Cl_9$[38] compounds and normal coordinate analysis[35,36,38] gave a complete assignment for the internal modes based on the $M_2X_9^{n-}$ complex with D_{3h} symmetry. The same symmetry was inferred for the $Zr_2Cl_9^-$ complex, based upon infrared and Raman spectra of the solid compound $[PBu^tCl_3][Zr_2Cl_9]$.[43]

The room-temperature spectra of polycrystalline $CsZr_2Cl_9$ (Fig. 6 and Table 4) show over 20 Raman bands. With increasing temperature the bandwidths increase, certain bands overlap, the lattice modes below ≈100 cm^{-1} succumb and thus in the spectra of the solid at ≈250 °C only seven bands can be seen (Fig. 6). These bands are assigned (Table 4) to the vibrational modes of the $Zr_2Cl_9^-$ complex species. The assignments are based on the previous work of $Cs_3Cr_2Cl_9$[36] and the assumption that $Zr_2Cl_9^-$ has D_{3h} symmetry. The metal–chloride terminal frequency for $Zr_2Cl_9^-$ and $Cr_2Cl_9^{3-}$ is very similar (≈380 cm^{-1}), but the ratio of bridging to terminal frequencies $\nu_b:\nu_t$ is 0.81 (Table 4) and 0.75:1[36] for Zr and Cr respectively. The higher ratio for Zr is justified from the high polarizing power of Zr relative to Cr.

The main features of the polycrystalline spectra at 250 °C are transferred to the melt spectra at 350 °C (Fig. 6). Two well defined polarized bands at 381 and 305 cm^{-1}, a polarized shoulder band at ≈365 cm^{-1} and three depolarized bands at 240, 160 and 117 cm^{-1} are recognized. The polarization characteristics of the bands at 381 and 305 cm^{-1} support their assignment to the ν_t and ν_b stretching frequencies of the $Zr_2Cl_9^-$ complex (Table 4). Further increase of the temperature does not change drastically the spectra; small frequency shifts and broadening of the bands occur but the strong polarized and depolarized bands as well as their relative intensities remain unchanged. All these observations indicate that the $Zr_2Cl_9^-$ is the predominant ionic species in the melt. The formation of such a species would stabilize the $ZrCl_4$ in the melt and thus the vapor pressure over molten $CsZr_2Cl_9$ is expected to be lower than that calculated by a gas–liquid equilibrium involving only the $ZrCl_6^{2-}$ and $ZnCl_4$ species. This accounts for the systematics of the vapor pressure data of Asvestas *et al.*[23]

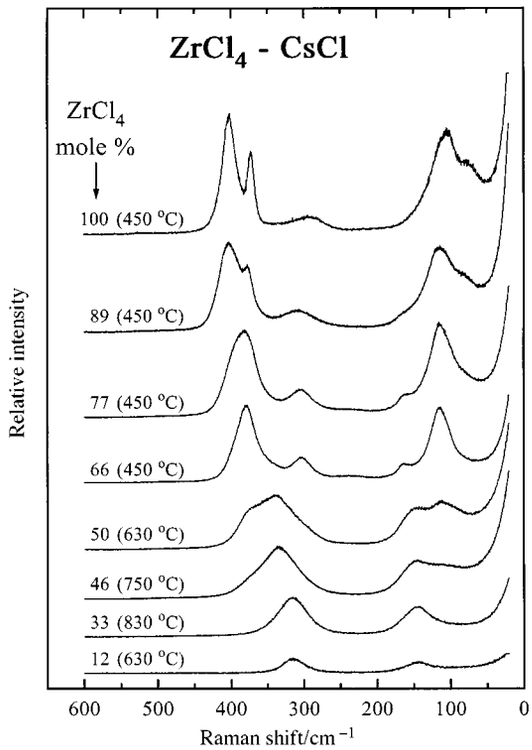

Fig. 7 Raman spectra of molten $ZrCl_4$–CsCl mixtures. Conditions similar to those in Fig. 1

Vibrational modes and structure of $ZrCl_4$–CsCl molten mixtures

The Raman spectra of $ZrCl_4$–CsCl mixtures have been measured at compositions x_{ZrCl_4} 0.05, 0.124, 0.203, 0.332, 0.457, 0.504, 0.553, 0.663, 0.769, 0.886 and 1.0 and at different temperatures above the liquidus ranging from 350 to 830 °C. Representative spectra are shown in Fig. 7 and the measured frequencies and proposed assignments are given in Table 5. For all measurements, identical light-scattering optical geometries, laser intensities and size of the fused-silica cell were used; this permitted less than 5% relative intensity measurements from different cells having a variety of melt compositions.

The phase diagram, the new $CsZr_2Cl_9$ compound observed (see above) and the overall behavior of the spectra (Fig. 7) suggest three composition regions where similarities or/and structural changes exist. These regions will be discussed separately.

The CsCl-rich region with $0 < x_{ZrCl_4} < 0.33$. This region concerns the pseudo-binary CsCl–Cs_2ZrCl_6 and the interpretation of the spectra is rather simple. At all compositions the spectra are similar to those of molten Cs_2ZrCl_6 and suggest that the predominant species in all these melts are the $ZrCl_6^{2-}$ octahedra. This view is further supported by measurements of the normalized (per mol of $ZrCl_4$) relative Raman intensity of the 320 cm^{-1} (A_1) mode of the octahedra, which was found to remain constant at all compositions studied ($x_{ZrCl_4} \leqslant 0.33$).

The bandwidth of the well defined 320 cm^{-1} band increases as expected with increasing temperature. At compositions very

Table 5 Raman shifts (cm^{-1}) observed[a] for molten $ZrCl_4$–CsCl mixtures. The numbers in square brackets are the full widths at half height (cm^{-1})

Composition (%)								
33.20 (830 °C)	45.7 (700 °C)	50.4 (630 °C)	55.3 (600 °C)	66.30 (450 °C)	76.7 (450 °C)	88.6 (450 °C)	100 (450 °C)	Assignment
						81 ± 3m (sh)	80 ± 2m (sh)	$(ZrCl_4)_n$
							107 ± 1s	$ZrCl_4$
	117 ± 3m (sh)	116 ± 2ms	114 ± 2s	116 ± 1vs	116 ± 1vs	115 ± 2s		$Zr_2Cl_9^-$
	148 ± 1s	147 ± 2m	148 ± 3m (sh)					$Zr_2Cl_{10}^{2-}/ZrCl_5^-$
148 ± 1s								$ZrCl_6^{2-}$
				165 ± 2mw	165 ± 4w (sh)	16 ± 3w (sh)		$Zr_2Cl_9^-$
			240 ± 5vw	238 ± 3w (br)	239 ± 4w			$Zr_2Cl_9^-$
							295 ± 2mw (p)	$(ZrCl_4)_n$
			305 ± 3mw (sh) (p)	305 ± 1m (p)	307 ± 1m (p)	308 ± 2m (p)		$Zr_2Cl_9^-$
320 ± 1vs (p)[50]								$ZrCl_6^{2-}$
							340 ± 5vw (p)	$(ZrCl_4)_n$
	335 ± 1vs (p)[64]	342 ± 1vs (p)[71]	342 ± 2ms (p)					$Zr_2Cl_{10}^{2-}/ZrCl_5^-$
				305 ± 5w (br)	355 ± 5w (br)			$Zr_2Cl_9^-$
							375 ± 1s (p)[13]	$ZrCl_4$
	377 ± 1vw (sh) (p)	377 ± 3w (sh) (p)	377 ± 2s (p)	380 ± 1vs (p) [36]	382 ± 2s (p) [37]	376 ± 2s (p) [22]		$Zr_2Cl_9^-$
						393 ± 2w (br)	398 ± 3w (br)	$(ZrCl_4)_n$
					400 ± 3w (sh) (p)	402 ± 2vs (p) [32]	404 ± 1vs (p) [23]	$(ZrCl_4)_n$

[a] s = strong, m = medium, w = weak, v = very, sh = shoulder, br = broad, p = polarized, dp = depolarized.

rich in CsCl the bandwidth is ≈35 cm^{-1} and increases at higher $ZrCl_4$ mole fractions reaching ≈50 cm^{-1} for the Cs_2ZrCl_6 melt. These changes reflect the stability and lifetime of the $ZrCl_6^{2-}$ octahedra in the melt mixtures. For melts very dilute in $ZrCl_4$ the well defined $ZrCl_6^{2-}$ octahedra are randomly distributed having mainly Cs^+ and Cl^- as nearest neighbors. The competition for the chloride anion between the tetravalent Zr^{4+} cation with a high polarizing power relative to monovalent Cs^+ cation yields stable and long-living $ZrCl_6^{2-}$ configurations. In contrast, at $ZrCl_4$ compositions close to 0.33 the melt is deficient in free chloride, the $ZrCl_6^{2-}$ octahedra are the main anions and more likely there is exchange of chloride anions between Zr^{4+} cations participating in neighboring octahedra; thus, relative to the dilute solutions, a decrease in the lifetime of the octahedra is expected and is consistent with the measured changes in the half width of the 320 cm^{-1} Raman band.

The region of the pseudo-binary Cs_2ZrCl_6–$CsZr_2Cl_9$. This region covers the compositions $0.33 < x_{ZrCl_4} < 0.66$ where drastic changes of the spectra occur (Fig. 7). Addition of $ZrCl_4$ to molten Cs_2ZrCl_6 gives rise to a new polarized band at 335–342 cm^{-1} which predominates at compositions up to $x_{ZrCl_4} \approx 0.4$ to 0.45. Further increase of $ZrCl_4$ leads to bands attributed to $Zr_2Cl_9^-$ as discussed above. It is evident from Fig. 7 that on going from the composition 0.33 in the $ZrCl_4$ mixture where the $ZrCl_6^{2-}$ octahedra are the predominant species to the 0.66 in the $ZrCl_4$ mixture characterized by the $Zr_2Cl_9^-$ face-sharing bi-octahedra we pass through one (or more) intermediate species having a strong polarized band at ≈340 cm^{-1} and a depolarized band at ≈150 cm^{-1}. Such species would have Zr : Cl mole ratios between the 'end' compositions 1 : 6 (*i.e.* $ZrCl_6^{2-}$) and 1 : 4.5 (*i.e.* $Zr_2Cl_9^-$). Obvious candidates would be the ions with stoichiometry ratios 1 : 5 and/or 1 : 5.5 corresponding to $ZrCl_5^-$, $Zr_2Cl_{10}^{2-}$ and/or $Zr_2Cl_{11}^{3-}$ respectively. The dimeric ions would have structures preserving the six-fold co-ordination of Zr where the octahedra share an edge ($Zr_2Cl_{10}^{2-}$; Fig. 3, **F**) or an apex ($Zr_2Cl_{11}^{3-}$; Fig. 3, **G**); thus on going from the free $ZrCl_6^{2-}$ octahedra of the 1 : 6 mixture to the phase-sharing octahedra $Zr_2Cl_9^-$ of the 1 : 4.5 mixture, intermediate structures are formed with increasing $ZrCl_4$ content where the octahedra are linked gradually by an apex, an edge and finally a face. However, a literature search indicated that highly charged polynuclear ions like $Zr_2Cl_{11}^{3-}$ are not commonly seen either in solid-state compounds or in condensed molten-salt systems. In contrast, species like $ZrCl_5^-$ (trigonal bipyramidal) and $Zr_2Cl_{10}^{2-}$ are well known for most tetravalent Group IVA elements; we thus assign the 340 cm^{-1} band observed in our spectra to one of these 1 : 5 species. Table 6 gives a collection of references for the chloride compounds of Zr and Ti which have established by X-ray crystallography and/or vibrational spectroscopy the formation of the 1 : 5 monomeric and dimeric ions. In Table 7 the metal–chloride 'terminal' frequencies for different titanium chloride species are compared with those observed for the corresponding zirconium compounds. The 340 cm^{-1} band of the 1 : 5 species is close to the 'terminal' frequencies expected for both $ZrCl_5^-$ and $Zr_2Cl_{10}^{2-}$ and thus no definite conclusions can be drawn for the structure of the predominant species in the melt mixture with $ZrCl_4$ mole fraction around 0.4.

Measurements of spectra at different temperatures have shown that, depending on the melt composition, the Raman intensities may or may not change. Thus, for the 'end' compositions Cs_2ZrCl_6 and $CsZr_2Cl_9$ the variation of temperature caused no drastic effect on the spectra; only slight frequency shifts and band broadening occurred. In contrast, for the

Table 6 Vibrational spectroscopy and X-ray data (*) available for compounds of Ti and Zr

Compound	A
$A_2Ti_2Cl_{10}$	NEt_4,[33] NPr_4,[33] PCl_4[33,34,44*]
$A_2Zr_2Cl_{10}$	$S_4N_xCl_y$[45*]
$ATiCl_5$	NBu_4,[33,46] $P(As)Ph_4$,[46] PCl_4[34,35]
$AZrCl_5$	NEt_4,[47*], $AsPh_4$,[48] PCl_4,[49] Cs[50*]

Table 7 Vibrational 'terminal' bands (cm^{-1}) of metal (Ti or Zr) chlorides species

M	MCl_4	MCl_5^-	MCl_6^{2-}	$M_2Cl_9^-$	$M_2Cl_{10}^{2-}$	M_2Cl_8
Ti	389[a]	350[b]	320[c]	420–380[d]	390–340[e]	
Zr[f]	375	340 (?)[g]	320	380	340 (?)[g]	404

[a] Ref. 17. [b] Refs. 33–35. [c] Refs. 26 and 34. [d] Refs. 33 and 35. [e] Refs. 33 and 35. [f] This work. [g] Alternative assignment.

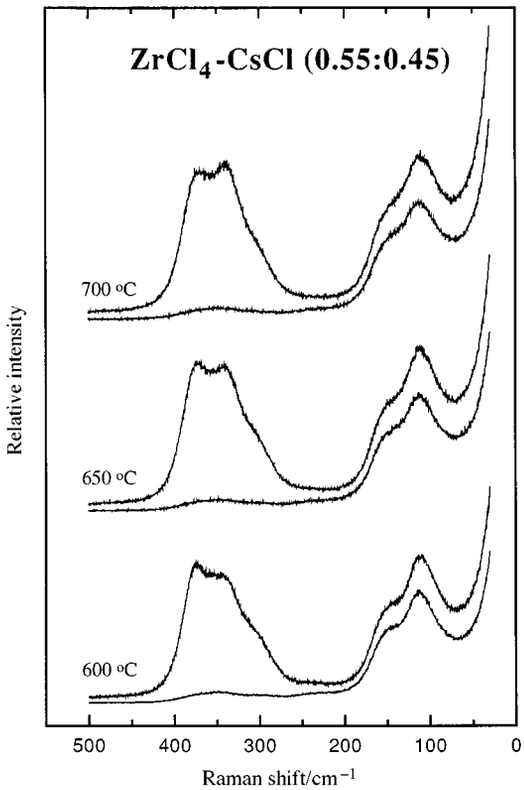

Fig. 8 Temperature dependence of the Raman spectra of the molten mixture $ZrCl_4$–CsCl ($x_{ZrCl_4} = 0.553$). Conditions as in Fig. 1

intermediate compositions the relative band intensities were found to change with temperature. This is clearly depicted in Fig. 8 for the mixture with $x_{ZrCl_4} = 0.55$ where the intensity of the 380 cm^{-1} band of the $Zr_2Cl_9^-$ species decreases, with increasing temperature, relative to the 340 cm^{-1} band of the $(ZrCl_5^-)_n$ species. This variation indicates that at least two zirconium species are in equilibrium, (6), where the n (= 1 or 2)

$$(ZrCl_5^-)_n \rightleftharpoons \tfrac{n}{2} Zr_2Cl_9^- + \tfrac{n}{2} Cl^- \qquad (6)$$

corresponds to the possible species $ZrCl_5^-$ and $Zr_2Cl_{10}^{2-}$. However, due to the high polarizing power of the Zr^{4+} ion, the presence of 'free' chloride ions in melt mixtures with composition $x_{ZrCl_4} > 0.33$ can be excluded and thus a third zirconium species should be involved in the above equilibrium. The most probable species is $ZrCl_6^{2-}$ possessing a polarized Raman band within the band contour of the other two species and being predominant at compositions near $x_{ZrCl_4} \approx 0.33$. Depending on the adopted structure of the 1 : 5 species, the equilibria (7) and (8) could reflect the spectral changes with temperature.

$$Zr_2Cl_9^- + ZrCl_6^{2-} \rightleftharpoons 3ZrCl_5^- \qquad (7)$$

$$Zr_2Cl_9^- + ZrCl_6^{2-} \rightleftharpoons \tfrac{3}{2} Zr_2Cl_{10}^{2-} \qquad (8)$$

The relative band intensities in Fig 8 suggest that the concentration of the $Zr_2Cl_9^-$ species decreases with increasing temperature; *i.e.* the enthalpies of the above equilibria (as written) are endothermic ($\Delta H_R > 0$). All ionic species in reaction (8) have the Zr in six-fold co-ordination and a small and probably positive enthalpy of reaction is expected due to the involvement of mainly bridging bond changes between the reactants and product. To a first approximation, reaction (8) involves six bridging bonds of the phase-sharing octahedra in $Zr_2Cl_9^-$ which change to six bridging bonds of the edge-sharing octahedra in $Zr_2Cl_{10}^{2-}$, while the number of terminal bonds does not change. Furthermore, this reaction is related to (7) through the exothermic dimerization (9), which implies that (7) is endothermic. In other words the temperature dependence of the

$$2ZrCl_5^- \rightleftharpoons Zr_2Cl_{10}^{2-} \qquad \Delta H_D < 0 \qquad (9)$$

spectra and the thermodynamic considerations support the presence of the monomeric $ZrCl_5^-$ species without excluding dimeric $Zr_2Cl_{10}^{2-}$. Accurate theoretical calculations of the enthalpies of reactions (7) and (8) might give a more conclusive answer and help in the assignment of the 340 cm^{-1} band.

The $ZrCl_4$-rich region with $0.66 < x_{ZrCl_4} \leqslant 1$. Addition of $ZrCl_4$ to the eutectic mixture ($x_{ZrCl_4} \approx 0.67$) gradually changes the spectra (Fig. 7). The $Zr_2Cl_9^-$ bands predominating in the eutectic mixture are preserved at higher $ZrCl_4$ compositions and at the same time bands due to $(ZrCl_4)_n$–$ZrCl_4$ liquid appear. It seems that in this $ZrCl_4$-rich composition range the spectra consist of a superposition of bands due to $(ZrCl_4)_n$, $ZrCl_4$ and $Zr_2Cl_9^-$ species.

If the average value of n for the polymer-like $(ZrCl_4)_n$ structure is large, then the addition of Cl^- (CsCl) to molten zirconium chloride, apart from the formation of $Zr_2Cl_9^-$ ions, is expected to break up the $(ZrCl_4)_n$ into smaller units *e.g.* $(ZrCl_4)_m$ with $m < n$. Thus a reaction scheme like (10) in combination

$$(ZrCl_4)_n + \left(\frac{n-m}{2}\right) Cl^- \rightleftharpoons (ZrCl_4)_m + \left(\frac{n-m}{2}\right) Zr_2Cl_9^- \qquad (10)$$

with the dissociation reaction (5) could account for the gradual spectral changes with composition (Fig. 7).

Measurements of the relative intensity of the 375 (monomer) to the 405 cm^{-1} (n-mer) bands for the mixture ($x_{ZrCl_4} = 0.89$) and the pure component ($x_{ZrCl_4} = 1$) show that the ratio I_{375}/I_{405} is not different for the two liquids. This indicates that the value of n is not much affected by the addition of Cl^- (*i.e.* $m = 0$). Such behavior is expected for non-polymer-like melts or for small n values and supports the view outlined above that hexamers and/or dimers in equilibrium with monomers are the predominant species in pure molten zirconium chloride.

Acknowledgements

We thank Yannis Bessiris for his help with computer-generated figures and graphics.

References

1 M. Brooker and G. N. Papatheodorou, *Adv. Molten Salt Chem.*, 1983, **5**, 27.
2 E. A. Pavlatou and G. N. Papatheodorou, *Proc. 8th Int. Symp. Molten Salts*, 1992, **92-16**, 72.
3 G. A. Voyiatzis and G. N. Papatheodorou, *Ber. Bunsenges. Phys. Chem.*, 1994, **98**, 683.
4 G. N. Papatheodorou, *J. Chem. Phys.*, 1977, **66**, 2893.
5 G. M. Photiadis, G. A. Voyiatzis and G. N. Papatheodorou, *Molten Salt Forum*, Trans. Tech. Publications Ltd. Aedermanusdorf, Switzerland, 1993, vols. 1 and 2, pp. 183–194.
6 L. M. Toth, A. S. Quist and G. E. Boyd, *J. Phys. Chem.*, 1973, **77**, 1384.
7 G. J. Kipouros, J. H. Flint and D. R. Sadoway, *Inorg. Chem.*, 1985, **24**, 3881.
8 B. Krebs, *Z. Anorg. Allg. Chem.*, 1970, **378**, 263; *Angew. Chem.*, 1969, **81**, 120; *Angew. Chem., Int. Ed. Engl.*, 1969, **8**, 146.
9 A. B. Salyulev and I. D. Kornyakova, *Rasplavy*, 1991, **6**, 95.
10 W. Brockner and A. F. Demiray, *J. Raman Spectrosc.*, 1978, **7**, 330.
11 A. B. Salyulev and I. D. Kornyakova, *Rasplavy*, 1994, **2**, 60; 1995, **6**, 58.
12 G. J. Kipouros and S. N. Flengas, *J. Electrochem. Soc.*, 1985, **132**, 1087.

13 G. J. Kipouros and S. N. Flengas, *Proc. 7th Int. Symp. Molten Salts*, 1990, **90-17**, 626.
14 W. J. Kroll, *J. Less-Common Met.*, 1965, **7**, 361.
15 S. Boghosian and G. N. Papatheodorou, *J. Phys. Chem.*, 1989, **93**, 415.
16 H. Schafer and M. Binnewies, *Z. Anorg. Allg. Chem.*, 1974, **410**, 251.
17 R. C. Taylor, E. M. Larsen and D. R. Taylor, *J. Inorg. Nucl. Chem.*, 1981, **43**, 293.
18 R. J. H. Clark, B. K. Hunter and D. M. Rippon, *Inorg. Chem.*, 1972, **11**, 56.
19 N. D. Denisova, E. K. Safronov and O. N. Bystrova, *Russ. J. Inorg. Chem.* (*Engl. Transl.*), 1966, **11**, 171.
20 L. A. Nisel'son and T. D. Sokolova, *Russ. J. Inorg. Chem.* (*Engl. Transl.*), 1962, **7**, 1382.
21 L. A. Nisel'son, V. I. Stolyarov and T. D. Sokolova, *Russ. J. Phys. Chem.* (*Engl. Transl.*), 1965, **39**, 1614.
22 I. S. Morozov and S. In-Chzhu, *Zh. Neorg. Khim.*, 1959, **4**, 680.
23 D. A. Asvestas, P. Pint and S. N. Flengas, *Can. J. Chem.*, 1977, **55**, 1154.
24 *Phase Diagrams for Ceramists*, compiled at the National Institute of Standards and Technology, edited and published by the American Ceramic Society, Westerville, OH.
25 H. D. B. Jenkins and K. F. Pratt, *Adv. Inorg. Chem. Radiochem.*, 1979, **22**, 1.
26 W. V. Bronswyk, R. J. H. Clark and L. Maresca, *Inorg. Chem.*, 1969, **8**, 1395.
27 G. N. Papatheodorou, *Inorg. Nucl. Chem. Lett.*, 1975, **11**, 483.
28 K. Nakamoto, *Infrared and Raman Spectra of Inorganic and Coordination Compounds*, 4th edn., Wiley, New York, 1986.
29 R. E. Hester, in *Raman Spectroscopy Theory and Practice*, ed. H. A. Szymanski, Plenum Press, New York, 1967.
30 L. A. Woodward and M. J. Ware, *Spectrochim. Acta*, *Part A*, 1963, **19**, 775.
31 B. Boressen, V. Dracoupoulos, G. Photiadis, B. Gilbert and G. N. Papatheodorou, *Proc. 10th Int. Symp. Molten Salts*, 1996, **96-7**, 11.
32 V. Dracopoulos, B. Gilbert, B. Boressen, G. Photiadis and G. N. Papatheodorou, *J. Chem. Soc.*, *Faraday Trans.*, 1997, 3081.
33 C. S. Creaser and J. A. Creighton, *J. Chem. Soc.*, *Dalton Trans.*, 1975, 1402.
34 A. F. Demiray and W. Brockner, *Spectrochim. Acta*, *Part A*, 1979, **35**, 659.
35 A. F. Demiray, W. Brockner, B. N. Cyvin and S. J. Cyvin, *Z. Naturforsch.*, *Teil A*, 1979, **34**, 362.
36 J. D. Black, J. T. R. Dunsmuir, I. W. Forrest and A. P. Lane, *Inorg. Chem.*, 1975, **14**, 1257.
37 R. Saillant, R. B. Jackson, W. E. Streib, K. Folting and R. A. D. Wentworth, *Inorg. Chem.*, 1971, **10**, 1453.
38 I. R. Beattie, T. R. Gilson and G. A. Ozin, *J. Chem. Soc. A*, 1968, 2765.
39 J. Beck, *Chem. Ber.*, 1991, **124**, 677.
40 L. Chen and F. A. Cotton, *Inorg. Chem.*, 1996, **35**, 7364.
41 R. J. Ziegler and W. M. Risen, jun., *Inorg. Chem.*, 1972, **11**, 2796.
42 M. M. Metallinou, L. Nalbandian, G. N. Papatheodorou, W. Voight and H. H. Emons, *Inorg. Chem.*, 1991, **30**, 4260.
43 J. I. Bullock, F. W. Parret and N. J. Taylor, *Can. J. Chem.*, 1974, **52**, 2880.
44 T. J. Kistenmacher and G. D. Stucky, *Inorg. Chem.*, 1971, **10**, 122.
45 J. Eicher, U. Muller and K. Dehnicke, *Z. Anorg. Allg. Chem.*, 1985, **521**, 37.
46 C. S. Creaser and J. A. Creighton, *J. Inorg. Nucl. Chem.*, 1979, **41**, 469.
47 T. G. Hughes, C. Meredith and J. Sutcliffe, *Inorg. Chim. Acta*, 1988, **143**, 209.
48 F. Esmadi and H. Sutcliffe, *Indian J. Chem.*, *Sect. A*, 1991, **30**, 99.
49 A. F. Demiray and W. Brockner, *Monatsh. Chem.*, 1980, **111**, 21.
50 J. Zhang and J. D. Corbett, *Inorg. Chem.*, 1995, **34**, 1652.

Received 2*nd October* 1997; *Paper* 7/07126D